

# UC San Diego

## UC San Diego Previously Published Works

### Title

Whistlerization and anisotropy in two-dimensional electron magnetohydrodynamic turbulence

### Permalink

<https://escholarship.org/uc/item/4dx8s29c>

### Journal

Physics of Plasmas, 7(2)

### ISSN

1070-664X

### Authors

Dastgeer, Sheikh  
Das, Amita  
Kaw, Predhiman  
[et al.](#)

### Publication Date

2000-02-01

### DOI

10.1063/1.873843

Peer reviewed

# Whistlerization and anisotropy in two-dimensional electron magnetohydrodynamic turbulence

Sheikh Dastgeer

*Institute for Plasma Research, Bhat, Gandhinagar, 382428, India*

Amita Das<sup>a)</sup>

*University of California at San Diego, La Jolla, California 92093*

Predhiman Kaw

*Institute for Plasma Research, Bhat, Gandhinagar, 382428, India*

P. H. Diamond

*University of California San Diego, La Jolla, California 92093*

(Received 17 August 1999; accepted 8 November 1999)

A detailed numerical simulation to understand the turbulent state of the decaying two-dimensional electron magnetohydrodynamics is presented. It is observed that the evolved spectrum is comprised of a collection of random eddies and a gas of whistler waves, the latter constituting the normal oscillatory modes of such a model. The whistlerization of the turbulent spectra has been quantified by novel diagnostics. In this work, results are presented only in the regime where the spatial excitation scales are longer than the electron skin depth. Simulations suggest that spectra at short scales are comparatively more whistlerized. The long scale field merely acts as the ambient field along which whistler waves propagate. It is also observed that, in the presence of an external magnetic field, the power spectrum acquires a distinct directional dependence. This anisotropy is dominant at short scales. It is shown that such an anisotropy at short scales results from a cascade mechanism governed by the interacting whistlers waves. © 2000 American Institute of Physics. [S1070-664X(00)04602-4]

## I. INTRODUCTION

The problem of turbulence has been studied both in the context of ordinary as well as magnetofluids. Progress in the study of the problem of turbulence in the magnetofluids (e.g., plasma) is comparatively recent and indicates interesting similarities and differences vis a vis ordinary fluids. One of the most important distinctions from the neutral, nonconducting fluids stems from the fact that magnetofluids, like plasmas can support a variety of waves. Turbulence in the magnetohydrodynamic (MHD) model, which supports dispersionless Alfvén waves as normal modes, has been explored in considerable detail. It is observed that in the case of MHD, the existence of these waves leads to subtle effects in turbulence. There are suggestions that there may be a modification in the power spectral index from that predicted on the basis of Kolmogorov's dimensional arguments. This is termed the Alfvén effect.<sup>1</sup> The interactions amongst the Alfvén waves are fairly restrictive, with only oppositely traveling waves interacting with each other. This results in strong anisotropy of the spectrum in the presence of external magnetic fields. The magnetohydrodynamics (MHD) model for plasma applies for the description of phenomena where the time scales are reasonably slow and the dynamics is mainly governed by the ion species. There exists another model which depicts MHD phenomena occurring at faster time scales; in this case ions do not have time to respond

because of their heavy mass and merely provide a neutralizing background, and the dynamics is entirely governed by the lighter electron species. Such a model is known as the electron magnetohydrodynamics (EMHD) model.<sup>2</sup> In contrast to MHD, this particular model supports dispersive waves known as whistlers. This model was more or less unexplored so far and has attracted interest lately due to its potential applications in fast switches, Z pinches, solar physics, magnetospheric reconnection, and ionospheric phenomena.<sup>2,3</sup> A recent numerical work by Biskamp *et al.*<sup>4,5</sup> on decaying EMHD turbulence has shown agreement with Kolmogorov's dimensional argument<sup>6</sup> for the scaling of power spectrum with wave number. On the basis of this result, they indicate that the whistler effect may not play any significant role in EMHD turbulence.

We define the concept of whistlerization of the turbulence viz. how closely the whistler mode relationship  $b_k = k\psi_k$  (physically an equipartition between the axial and poloidal magnetic energies) is obeyed in the turbulent state. As stated previously, the power spectral index in EMHD turbulence does not seem to be significantly influenced by the whistler effect. However, whistlerization does take place, as evidenced by the simulations of Biskamp *et al.*,<sup>4,5</sup> who have shown that at longer scales than the skin depth ( $kd_e < 1$ ) there is significant equipartition between the axial and poloidal magnetic energies. One of the objectives of the present work is to understand the degree of whistlerization of the turbulent state in EMHD in quantitative detail. For this pur-

<sup>a)</sup>Permanent address: Institute for Plasma Research, Gandhinagar, India.

pose, we seek to address the following issues in the subsequent sections; (i) quantification of the extent of whistlerization of the spectra, (ii) scale dependence of whistlerization, (iii) dependence of whistlerization on the strength of external field, and (iv) time evolution of a random initial spectra toward a whistlerized state. Another objective is to study the influence of an external magnetic field on the spectrum, and the reasons thereof. For this we would largely explore (i) the characteristic difference in the spectrum in directions parallel and perpendicular to the external field (e.g., anisotropy in the spectrum) and (ii) scale dependence of anisotropy, etc.

The paper is organized as follows. In Sec. II we discuss briefly the EMHD model and the numerical results on whistlerization. We conclude that the turbulence evolves toward a state comprised of a mixture of a gas of whistler waves (interacting randomly with each other) and a collection of random eddies. The tendency for whistlerization seems to be stronger at shorter scales in the inertial range. Basically, the long scale field acts as an ambient magnetic field along which the short scale whistler perturbations propagate. Numerical studies of the spectrum in the presence of external magnetic field are presented in Sec. III. In the presence of an external magnetic field, we observe that the spectrum acquires directional dependence. It is observed that the perpendicular scales are predominantly shorter in comparison to parallel scales. Furthermore, this disparity in parallel and perpendicular scales is stronger at shorter scale lengths. It seems quite likely that the observed anisotropy arises as a result of interactions amongst whistler waves, which primarily propagate parallel to the magnetic field. In Sec. IV we provide a theoretical understanding of observed anisotropy in the power spectrum on the basis of whistler wave interactions. Section V contains the conclusion.

## II. WHISTLERIZATION IN EMHD TURBULENCE

Electron magnetohydrodynamics (EMHD) is the description of electromagnetic phenomena in a magnetized plasma at fast time scales where only electron dynamics is important. Ions merely provide a stationary neutralizing background. The EMHD model has been discussed in considerable detail in some of the earlier works.<sup>2,4,5,7,8</sup> Here, we concentrate on the case when the electromagnetic perturbations vary only in two dimensions, e.g., the  $x$ - $y$  plane. The EMHD model is then represented by the following set of coupled equations in the two fields  $b$  and  $\psi$ .

$$\frac{\partial}{\partial t}(\psi - \nabla^2 \psi) + \hat{z} \times \nabla b \cdot \nabla(\psi - \nabla^2 \psi) = \eta \nabla^2 \psi, \quad (1)$$

$$\frac{\partial}{\partial t}(b - \nabla^2 b) - \hat{z} \times \nabla b \cdot \nabla \nabla^2 b + \hat{z} \times \nabla \psi \cdot \nabla \nabla^2 \psi = \eta \nabla^2 b. \quad (2)$$

The total magnetic field can be expressed in terms of these fields as  $\mathbf{B} = \hat{z} \times \nabla \psi + b \hat{z}$ . The two evolution equations have been written in normalized variables. The length scales are normalized by the electron skin depth  $d_e = c/\omega_{pe}$ , magnetic field by a typical amplitude  $B_0$  and time by the corresponding electron gyrofrequency. The dispersion relation for whis-

tlers, the normal mode of oscillation in the EMHD frequency regime, can be obtained by linearizing Eqs. (1) and (2) in the presence of uniform magnetic field  $B_{0y}$  pointing in the  $y$  direction as

$$\omega = \sigma \frac{k k_y B_{0y}}{(1 + k^2)}.$$

Here  $\sigma = \pm$  and indicates the direction of propagation. The whistler wave excitation leads to a coupling of the form  $b_k = \sigma k \psi_k$  between the two perturbed fields. It is interesting to note that the above-mentioned relation leads to an equipartition between the poloidal and the axial components of the magnetic/kinetic energies. This should be contrasted with MHD where the Alfvén wave excitation leads to an equipartition between magnetic and kinetic energies. There can be no equipartition between magnetic and kinetic energies as a result of whistlerization of the spectrum. The dominance of magnetic or kinetic energy is dependent on whether the typical turbulent scales of excitation are longer or shorter than the electron skin depth. Also, unlike Alfvén waves, these waves are dispersive. They propagate obliquely to the external magnetic field with a group velocity

$$\mathbf{V}_g = \frac{\sigma B_{0y} k_y k_x (1 - k^2)}{k(1 + k^2)^2} \hat{x} + \frac{\sigma B_{0y} [k^2(1 + k^2) + k_y^2(1 - k^2)]}{k(1 + k^2)^2} \hat{y}.$$

We now carry out numerical investigations to understand the turbulent state in EMHD. For this purpose we evolve the two fields  $b$  and  $\psi$  numerically using Eqs. (1) and (2), respectively, with the help of a fully de-aliased pseudospectral scheme. In this scheme the fields  $b$  and  $\psi$  are Fourier decomposed. Each of the Fourier modes are then evolved, the linear part exactly, whereas the nonlinear terms are calculated in real space and then Fourier transformed in  $k$  space. This requires going back and forth in real and  $k$  space at each time step. The fast Fourier transform (FFT) routines are used to go back and forth in the real and  $k$  space at each time integration. The time stepping is done using a predictor corrector with the midpoint leap frog scheme. Some test simulations were carried out at a lower resolution of  $128 \times 128$ . However, most results that we present here correspond to the resolution of  $256 \times 256$  and  $512 \times 512$  modes. For numerical studies the dissipation operator of Eqs. (1) and (2) were replaced by higher powers of Laplacian (cubic) in order to restrict dissipative effects at shorter scales. The typical values of the dissipation parameter  $\eta$  were chosen to lie between  $5 \times 10^{-1}$  to  $5 \times 10^{-2}$  in the various runs. The initial spectrum of the two fields  $b$  and  $\psi$  is chosen to be concentrated on a band of scales and their phases are taken to be random. The Fourier modes of the two fields are chosen to be entirely uncorrelated to begin with. Furthermore, in the present work we have chosen to restrict our studies to scales  $k d_e \lesssim 1$  where wave propagation effects are comparatively stronger.

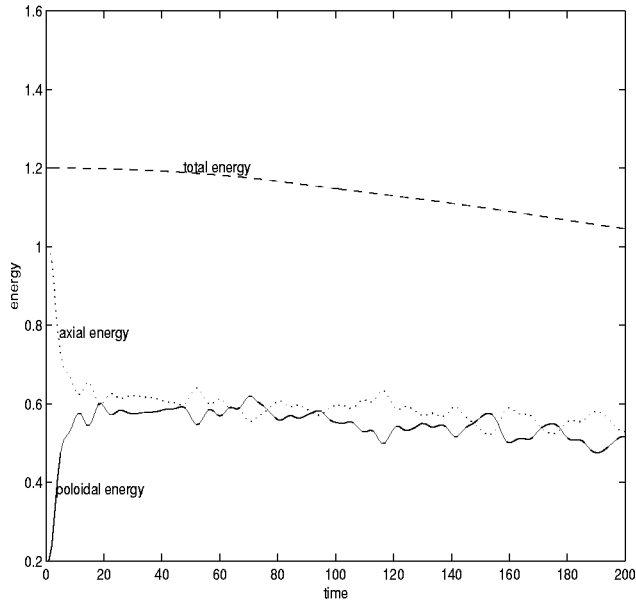


FIG. 1. The evolution of total energy (dashed line), axial ( $b$ ) field energy (dotted line), and the poloidal ( $\psi$ ) field energy (solid line) when the initial axial energy was greater than the poloidal energy.

The initial energy is distributed unequally in the poloidal  $\psi$  and axial  $b$  fields. In Figs. 1 and 2 we show the evolution of total energy (dashed line), and the energy in the fields  $b$  and  $\psi$ , which has been termed as axial and poloidal energies, respectively. The plots in Fig. 1 are for the case where the initial axial energy is chosen to be greater than the poloidal energy. We observe that the axial energy decays and the poloidal energy grows so as to achieve equal distribution of energies, in the two fields, ultimately. Figure 2 depicts the other scenario wherein the initial poloidal energy is larger than that in the axial field. In this case, the poloidal energy reduces and the axial energy increases with time, so that

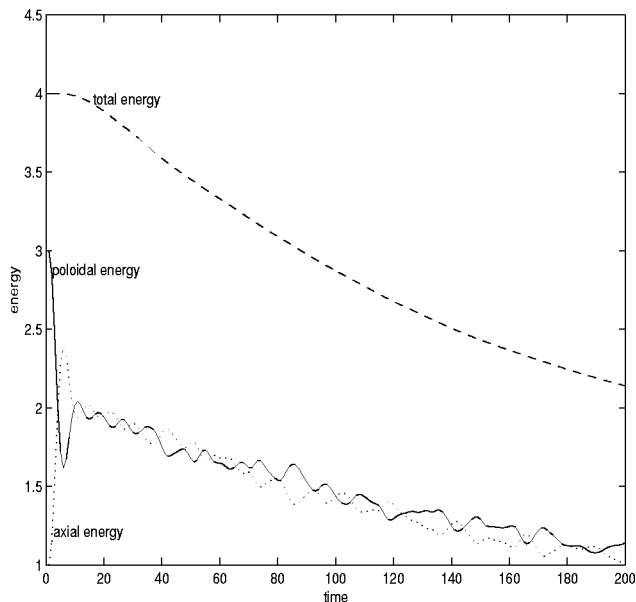


FIG. 2. Similar to Fig. 1, however, for this case the initial poloidal energy was chosen to be larger than the axial energy.

finally both acquire similar values. This shows that the energies associated with the two fields strive to achieve equipartition.

A complete whistlerization of the turbulent spectra, i.e., when the spectrum is comprised of a collection of randomly phased whistlers interacting with each other, will automatically lead to an equal distribution of energy in the axial and poloidal fields. This is so because the relationship,  $b_k = \pm k \psi_k$ , is satisfied for whistler modes. However, one cannot infer the opposite, i.e., from the observed equality of poloidal and axial energies it cannot be concluded with certainty that the spectrum is completely whistlerized. This is so because the axial and poloidal energies represent integral quantities, where contribution from each mode has been summed. Thus to ensure the extent to which the relationship  $b_k = \pm k \psi_k$  is satisfied for each of the individual modes, we introduce a set of new diagnostics, which are monitored during the course of numerical simulations. We define

$$\Omega_1(t) = \frac{1}{\sum_{k_x, k_y} \sum_{k_x, k_y} \frac{\text{abs}(|b_k|^2 - k^2 |\psi_k|^2)}{(|b_k|^2 + k^2 |\psi_k|^2)}}$$

to represent the extent of whistlerization of the spectrum. It is clear that for a completely whistlerized state  $\Omega_1$  will vanish. The more the state is whistlerized, the lower the value of  $\Omega_1(t)$ . In the definition of  $\Omega_1$  we have summed suitably normalized nonwhistlerized contribution of power from each mode. The contribution from each mode is normalized by its own spectral content. This treats all the modes on an equal footing. However, an alternative definition of the kind

$$\Omega_2(t) = \frac{\sum_{k_x, k_y} \text{abs}(|b_k|^2 - k^2 |\psi_k|^2)}{\sum_{k_x, k_y} (|b_k|^2 + k^2 |\psi_k|^2)}$$

can also be employed, where contribution from each mode is normalized by the average power. This definition selectively gives importance to modes having higher spectral power.

The evolutions of  $\Omega_1$  and  $\Omega_2$  are shown in Figs. 3 and 4, respectively, for various values of the external field  $B_0$ . The following points are clearly evident from the plot of  $\Omega_1$ . (i)  $\Omega_1$  rapidly decreases from its initial value and attains a statistically steady value, which is relatively small. This confirms the tendency for whistlerization of the spectrum, which happens even when the external field is absent. (ii) The asymptotic value of  $\Omega_1$  decreases with increasing magnetic field. Thus, the extent up to which a spectrum is whistlerized is dependent on the strength of magnetic field. (iii) The rate of whistlerization increases with magnetic field, the initial drop to the asymptotic value can be seen to be steepest for  $B_0 = 4$ , and gets shallower with decreasing value of  $B_0$ . It is also apparent that the asymptotic value of  $\Omega_1(t)$  shows fluctuations in time. These fluctuations are more rapid with increasing external fields. It appears that the time scale for the spectrum to get whistlerized, as well as its statistical behavior, are linked with a typical whistler time scale defined by the magnetic field strength and a suitably averaged spatial scale [e.g.,  $\tau_{\text{whistler}} \sim 1/(k_{\text{av}} \mathbf{k}_{\text{av}} \cdot \mathbf{B})$ ].

A comparison of the two plots of  $\Omega_1$  and  $\Omega_2$  draws attention to another interesting feature. It is clear that  $\Omega_2$  is

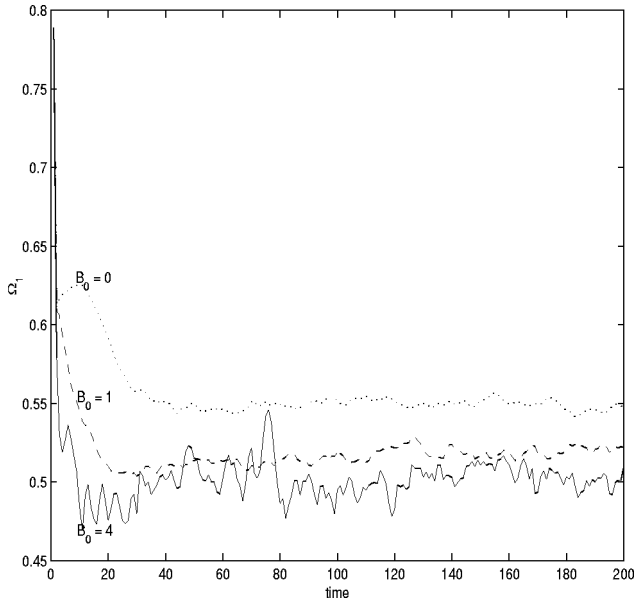


FIG. 3. Evolution of  $\Omega_1$  for  $B_0=0$  (dotted line),  $B_0=1$  (dashed line), and  $B_0=4$  (continuous).

always larger than  $\Omega_1$ . Since  $\Omega_2$  represents modes having higher spectral power, a comparative higher value of  $\Omega_2$  indicates that modes having higher spectral powers are less whistlerized. Since the power spectrum decays as  $k^{-7/3}$ , this also suggests that the large scale regime of the spectrum is less whistlerized. This clearly suggests that whistlerization occurs predominantly at short scales. We provide further evidence of the short scale part of the spectrum being more whistlerized in Fig. 5. The various plots of Fig. 5 show the evolution of a function similar to  $\Omega_1$  in which only certain scales in the summation have been included. Results have been shown both at the resolution of  $256 \times 256$  [Figs. 5(a) and 5(b)] and at  $512 \times 512$  [Figs. 5(c) and 5(d)]. In Figs. 5(a) and 5(c) and Figs. 5(b) and 5(d) we have chosen to plot the

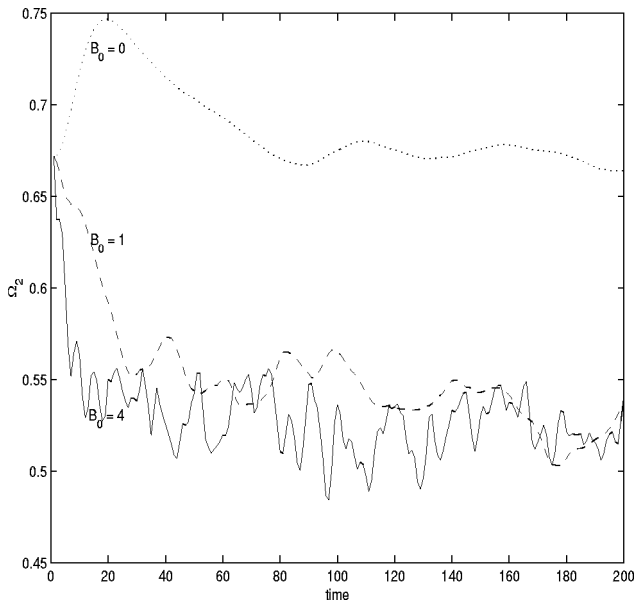


FIG. 4. Similar to Fig. 3, but showing evolution of  $\Omega_2$ .

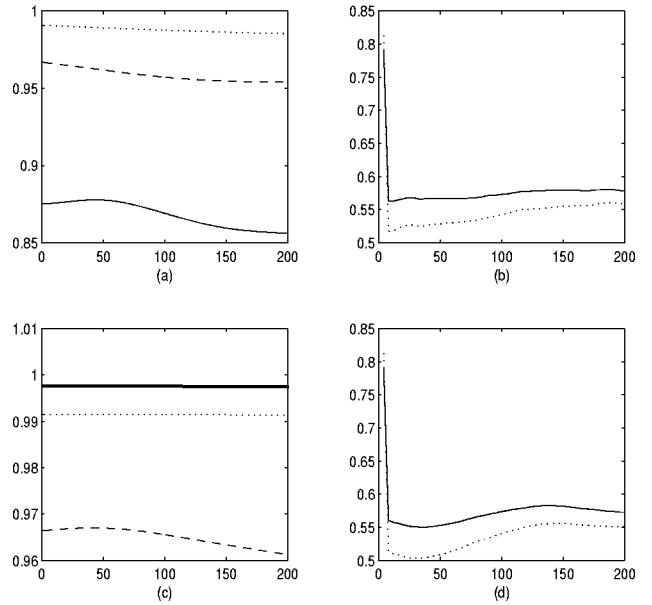


FIG. 5. Evolution of  $\Omega_1$  with contributions in the summation only from certain regions of scales. (a) and (b) Results for a resolution of  $256^2$ . (c) and (d) Results at  $512^2$ . For the dotted, dashed, and solid lines of (a) the scale lengths  $|k|$  included in the sum lie in the range  $0 \leq |k| < 2k_1$ ,  $0 \leq |k| < 4k_1$  and  $0 \leq |k| < 8k_1$  respectively, where  $k_1 = 0.0125$ . The scale lengths in the thick solid, dotted, and dashed lines of (c) lie in the range  $0 \leq |k| < 2k_2$ ,  $0 \leq |k| < 4k_2$  and  $0 \leq |k| < 8k_2$ , respectively, where  $k_2 = 0.00625$ . The solid lines of (b) and (d) represent the case when all the scales have been summed, however, the dashed lines of both (c) and (d) are when the scale lengths lie in the regime  $1/3k_{\max} \leq |k| < 2/3k_{\max}$ . Here  $k_{\max} = 1.6$  and  $2/3k_{\max}$  basically is the shortest scale available after aliasing.

evolution of  $\Omega_1$  containing contributions typically from long and short scales alone, respectively. As can be seen the typical values in Figs. 5(a) and 5(c) are closer to unity when compared with Figs. 5(b) and 5(d). It is also evident from the plots that as one successively incorporates contributions from shorter scales the value of the function  $\Omega_1$  keeps reducing. Furthermore, this inference holds consistently even as we increase the resolution from  $256^2$  to  $512^2$ . Thus it can be stated that the extent of whistlerization is greater at short scales. This is reasonable as the large scale fields merely act as an effective ambient magnetic field along which the whistlers propagate. We would, however, like to point out that the short scales for which we are drawing inferences here are typically longer than the electron skin depth.

It should be noted here that the linear whistler frequency  $\omega_{\text{lin}} = k\mathbf{k} \cdot \mathbf{B}$  is larger at short scales. Hence, the conditions for applicability of weak turbulence theory viz.  $\omega_{\text{lin}} \gg \Delta\omega_{\text{NL}}$  (where  $\Delta\omega_{\text{NL}}$  represents the nonlinear broadening of the modes) are more likely to be satisfied at short scales. Thus at short scales linear wave physics dominate and the small scale modes may be viewed as whistler wavepackets, whereas long scales are effectively magnetic eddies.

### III. SPECTRAL ANISOTROPY IN THE PRESENCE OF EXTERNAL MAGNETIC FIELD

In this section we study the evolution of the spectral properties of decaying EMHD turbulence in the presence of an external magnetic field. It is well known that the presence



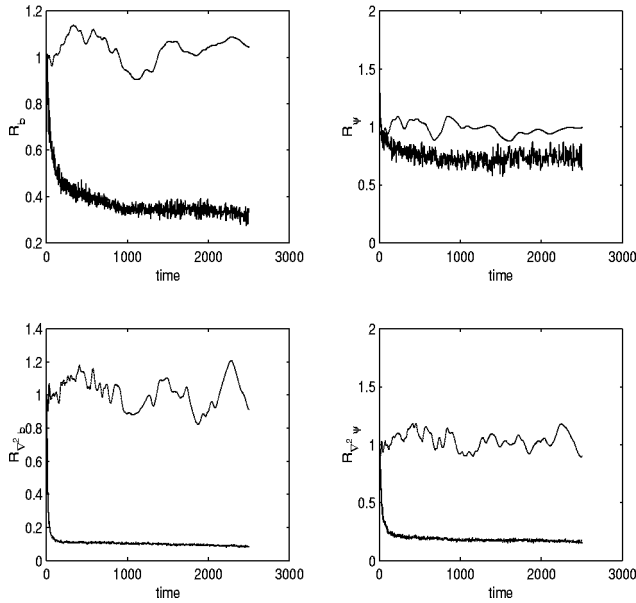


FIG. 6. Evolution of  $R$ , the anisotropy factor for the variables  $b$ ,  $\psi$ ,  $\nabla^2 b$ , and  $\nabla^2 \psi$ . The upper curve hovers around unity for the case when there is no imposed external field  $B_0=0$ ; the lower curve represents the case when  $B_0=7.5$ .

of a uniform magnetic field in the context of MHD gives rise to an anisotropic spectrum.<sup>9,10</sup> The power spectrum of the various variables in the case of MHD are known to show distinct directional dependence. This is clear from the MHD simulations carried out by Shebalin *et al.*<sup>9</sup> and most recently by Oughton *et al.*<sup>10</sup> It is believed that this happens primarily due to the excitation of Alfvén waves which preferentially propagate parallel to the external magnetic field, and hinder the process of spectral cascade parallel to the external field. This results in the anisotropy of the spectrum. Thus the origin of anisotropy is basically the restrictive interactions of the Alfvén waves for which only oppositely traveling waves interact. In the absence of external magnetic field, Alfvénic excitations are generated along the long scale turbulent field (which has a random orientation, and hence is isotropic). These Alfvénic excitations restrict the cascade mechanism and are also responsible for the deviation of power spectrum index from the Kolmogorov value of  $-5/3$  to a value  $-3/2$ .<sup>1,11</sup>

In the context of EMHD turbulence, it has been noted that the whistler effect on spectral index is negligible.<sup>4,5</sup> The numerically observed spectral index can be explained purely on the basis of Kolmogorov's dimensional arguments, without invoking any role, whatsoever, for the whistler waves. A natural question then arises whether in EMHD turbulence the spectrum is maintained isotropic even in the presence of a strong external magnetic field. This is what we intend to study in this section. We have seen in Sec. II that in the turbulent EMHD state both whistlers and random eddies co-exist. We have also seen indications that in the presence of external magnetic field the spectrum becomes more whistlerized, and that the short scale part of the spectrum shows stronger tendencies toward whistlerization. The intriguing question in this regard is whether these whistlers have any

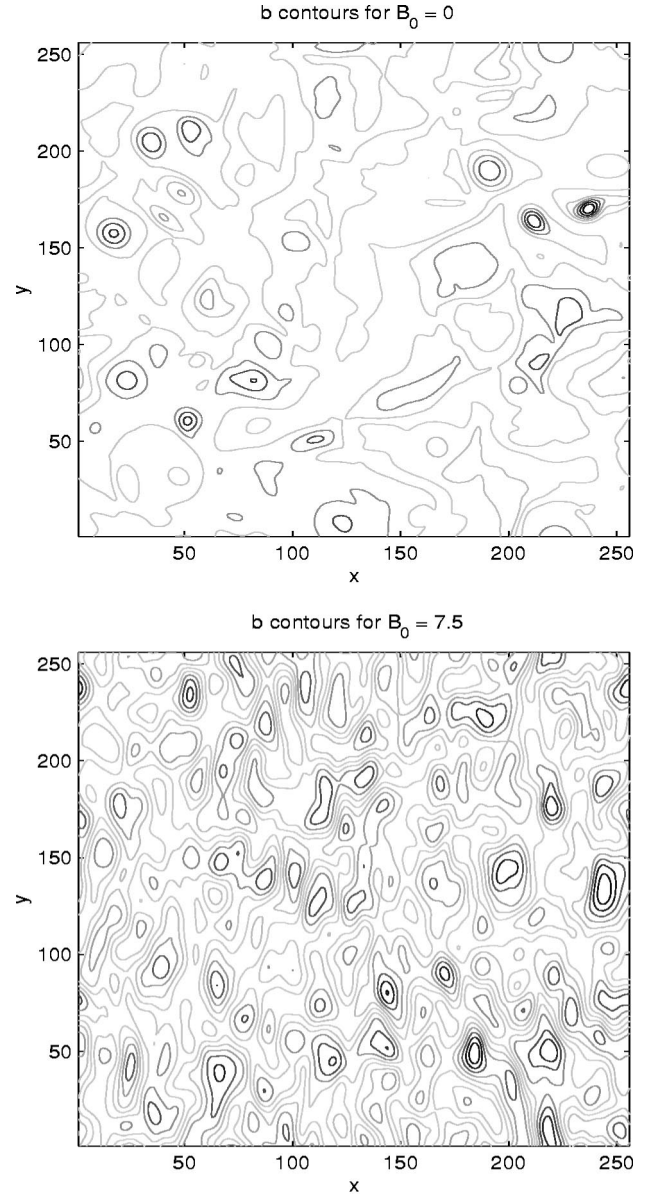


FIG. 7. Contour plots for the variable  $b$  in the evolved state for  $B_0=0$  and  $B_0=7.5$ .

role to play in the cascade mechanism. For this purpose we would like to investigate the spectral properties of the two fields  $b$  and  $\psi$  in the presence of varying external magnetic field. We would also like to investigate a possible distinction between short and long scales with regard to the anisotropization of the spectrum.

The numerical scheme has already been outlined in Sec. II. We have chosen the external magnetic field  $B_0$  to be along the  $y$  axis in our numerical studies. We then define the following ratio:

$$R_Q(t) = \frac{\sum_{k_x} \sum_{k_y} k_y^2 |Q(k_x, k_y, t)|^2}{\sum_{k_x} \sum_{k_y} k_x^2 |Q(k_x, k_y, t)|^2}. \quad (3)$$

Here,  $Q$  stands for any one of the following variables  $b$ ,  $\psi$ ,  $\nabla^2 b$ , and  $\nabla^2 \psi$ . It is clear that if the spectrum of  $Q$  is isotro-

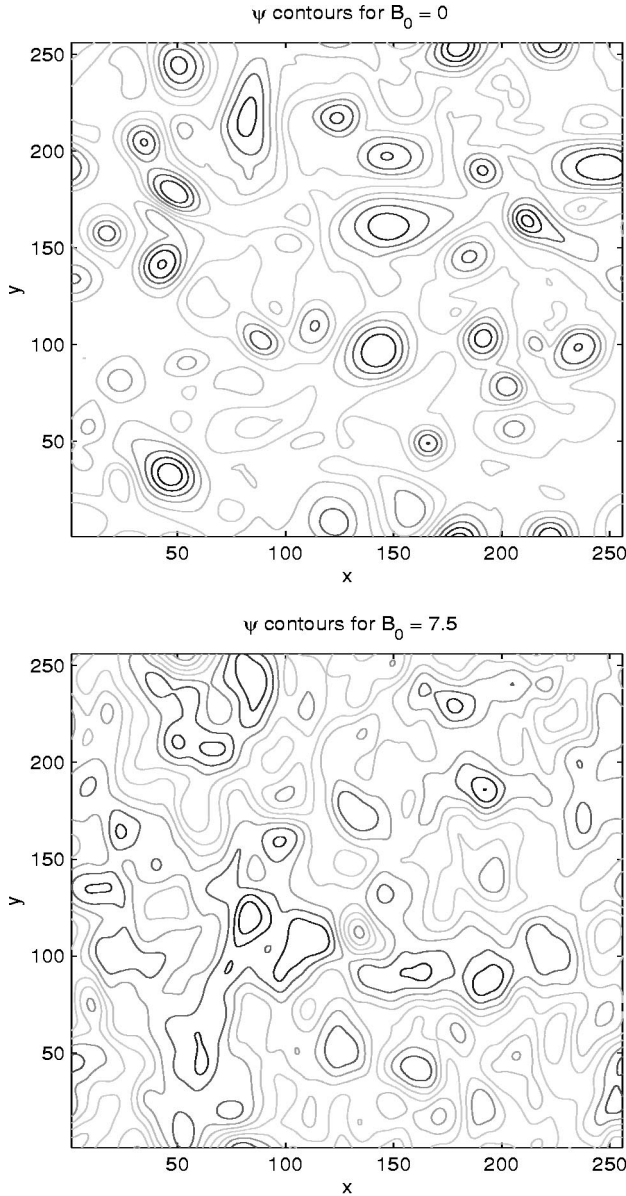


FIG. 8. Contour plots for the variable  $\psi$  in the evolved state for  $B_0=0$  and  $B_0=7.5$ .

pic then the ratio  $R_Q$  will be close to unity. Any deviation from unity is an indication of anisotropy in the spectrum.

The evolution of  $R_Q$  for the variables  $b$ ,  $\psi$ ,  $\nabla^2 b$ , and  $\nabla^2 \psi$  is shown in the four plots of Fig. 6. The upper curve in all these plots, which hovers around unity, is for  $B_0=0$ . As expected, it testifies to the fact that the spectrum of all the variables remains isotropic in the absence of any external magnetic field. The lower curve is for the case when the external magnetic field has been chosen to be  $B_0=7.5$ . It can be seen that the value of  $R$  corresponding to all the four variables drops off from unity and saturates at a low value. The plots also show that  $R_{\nabla^2 b}$  and  $R_{\nabla^2 \psi}$  saturate at a much lower value than compared with  $R_b$  and  $R_\psi$ , respectively. This clearly implies that the spectral anisotropy in the variables  $b$  and  $\psi$  is dominant at shorter scales. Furthermore, it is also evident that finally  $R_\psi > R_b$ , suggesting that the spectrum of  $b$  is more anisotropic compared to that of  $\psi$ . Since

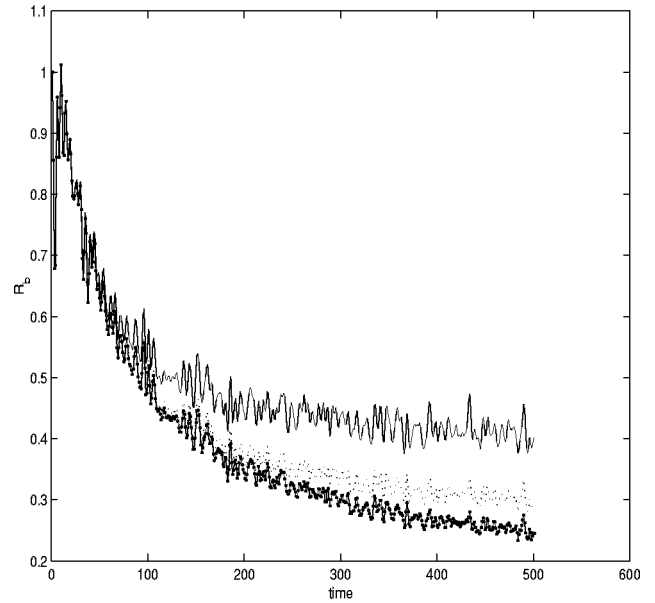


FIG. 9. Evolution of  $R_b$  for varying  $\eta$ , the dissipation parameter,  $\eta=0.05$  for the dotted line,  $\eta=0.005$  for the solid line, and  $\eta=0.0005$  for the dotted solid line.

the magnetic scalar potential  $\psi$  is known to cascade toward longer scales, the weak anisotropy observed in its spectrum can be attributed to the dominance of long scales in it.

The definition of  $R$  involves a numerator which is weighted by  $k_y^2$ , corresponding to the wave vector parallel to the direction of external magnetic field, whereas the denominator contains  $k_x^2$ , the perpendicular wave vector, as the factor inside the summation. Since  $R$  asymptotes toward a value lower than unity, it is obvious that the spectrum is evolving so as to have comparatively shorter scales perpendicular to the magnetic field. The contour plot of the variable  $b$  in the  $x$ - $y$  plane depicted in Fig. 7 clearly exemplifies the dominance of short scales perpendicular to the external magnetic field in the spectra of  $b$ . For,  $\psi$ , which exhibits comparatively weak anisotropy, the dominance of short scales perpendicular to the magnetic field cannot be gauged directly from its contour plot (e.g., Fig. 8).

We also observe that by reducing the value of  $\eta$ , the dissipation parameter results in an increased anisotropy of the spectrum. Figure 9 shows the evolution of  $R$  for the variable  $b$  for varying values of  $\eta$ . This can be understood by realizing that decreasing  $\eta$  is tantamount to pushing the dissipation scale toward shorter scales. Thus the short perpendicular scales generated in the cascade continue to survive in a larger domain of scales, as  $\eta$  is reduced, thereby  $R$  reduces further.

We define the average perpendicular and parallel scales as

$$\langle k_{\parallel}^2 \rangle = \frac{\sum_{k_x, k_y} k_y^2 Q(k_x, k_y, t)^2}{\sum_{k_x, k_y} Q(k_x, k_y, t)^2},$$

$$\langle k_{\perp}^2 \rangle = \frac{\sum_{k_x, k_y} k_x^2 Q(k_x, k_y, t)^2}{\sum_{k_x, k_y} Q(k_x, k_y, t)^2}.$$

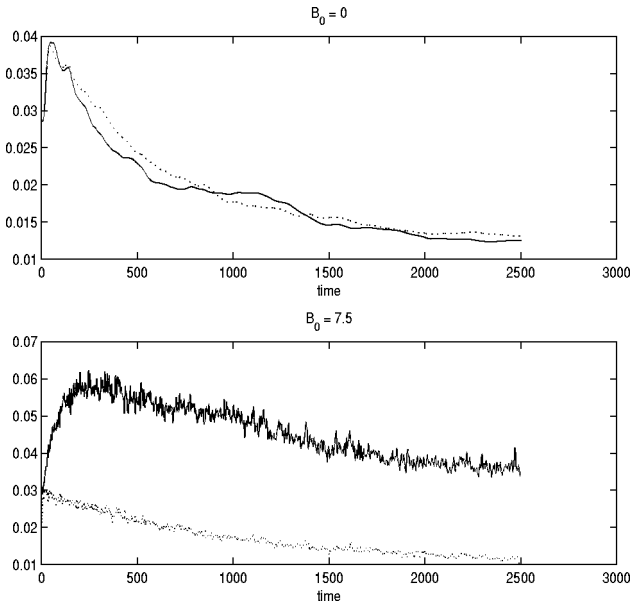


FIG. 10. Evolution of the average perpendicular (solid line) and parallel scales (dotted line) for the variable  $b$ .

Figures 10 and 11 show the evolution of the average perpendicular and the parallel scales for  $b$  and  $\psi$ , respectively. It is clear from the plots that average scale lengths for  $b$  are smaller in comparison to those of  $\psi$ . When  $B_0$  is finite there is a greater disparity between the perpendicular and parallel scales of  $b$  in comparison to  $\psi$ , with perpendicular scale lengths being shorter compared to parallel scales. Figure 10 shows that in the presence of finite external magnetic field  $B_0$ ,  $\langle k_{\perp}^2 \rangle$  for  $b$  shows steady rise initially. This tendency, however, does not continue forever. Rather, the curve subsequently flattens out and later exhibits the same slowly decaying tendency as that of the parallel scales. However, a distinct disparity between the perpendicular and parallel scales persists.

#### IV. THEORETICAL DISCUSSION

We would now like to understand what causes the anisotropy in the spectrum in the presence of external magnetic field, and why it is that it leads to a generation of short scales preferentially in the perpendicular direction. It should be mentioned at the outset, that unlike MHD, where the explanation for anisotropy is premised on an outright absence of certain kind of interactions amongst the Alfvén waves, here one can at best hope to provide an argument based on notions of more/less likelihood of certain interactions amongst whistlers. This is primarily because the whistlers, unlike Alfvén waves, are dispersive in nature.

It is clearly evident from the numerical results of Secs. II and III that the observed anisotropy and the whistlerization of the spectrum are related issues. Both occur preferentially at short scales. In this section we describe how whistlerization could possibly be responsible for the ensuing anisotropy in the spectrum in the presence of an external magnetic field.

For this purpose we first try to understand the nonlinear

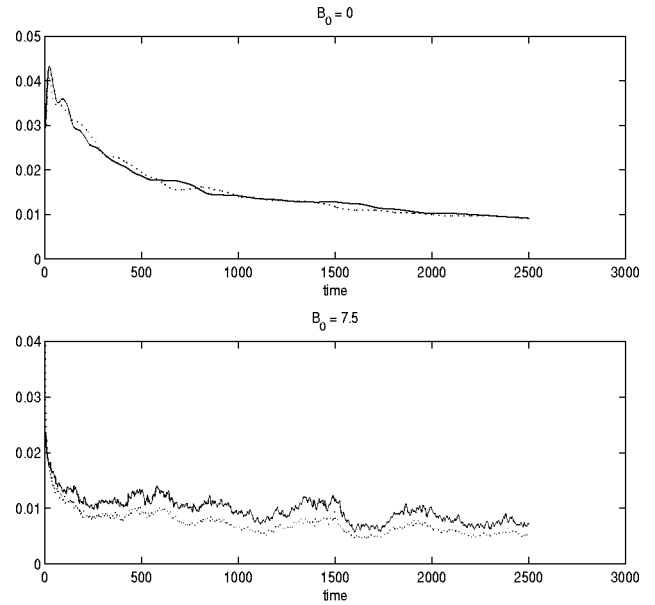


FIG. 11. Evolution of the average perpendicular (solid line) and parallel scales (dotted line) for the variable  $\psi$ .

interaction amongst the whistler waves. The EMHD equations in the  $kd_e \ll 1$  limit can be written as

$$\frac{\partial \mathbf{B}}{\partial t} + \mathbf{v}_e \cdot \nabla \mathbf{B} = \mathbf{B} \cdot \nabla \mathbf{v}_e. \quad (4)$$

Here  $\mathbf{v}_e = -\nabla \times \mathbf{B}$  is the electron velocity. Linearization of Eq. (4) in the presence of an external magnetic field in the  $y$  direction leads to the usual dispersion relation for whistlers, e.g.,  $\omega_k = \sigma_k k k_y B_0$ , along with the relationship  $\mathbf{v}_{ek} = -\sigma_k k \mathbf{B}_k$ . Here  $\sigma_k = \pm 1$  and refers to the direction of propagation of the  $k$ th mode. Now, Fourier analyzing Eq. (4) leads to

$$\frac{\partial \mathbf{B}_k}{\partial t} + \sum_{k_1} (\mathbf{v}_{e_{k-k_1}} \cdot i\mathbf{k}_1 \mathbf{B}_{k_1} - \mathbf{B}_{k-k_1} \cdot i\mathbf{k}_1 \mathbf{v}_{e_{k_1}}) = 0.$$

Substituting the linearized expression for  $\mathbf{v}_{e_{k-k_1}}$  we obtain

$$\frac{\partial \mathbf{B}_k}{\partial t} = \sum_{k_1} i\mathbf{k}_1 \cdot \mathbf{B}_{k-k_1} \mathbf{B}_{k_1} (\sigma_{k-k_1} |k-k_1| - \sigma_{k_1} |k_1|).$$

According to Kolmogorov's theory for fluid turbulence the triad of wave vectors forming the sides of an equilateral triangle are best suited for efficient power cascade. Assuming that this holds even for the case of EMHD turbulence, the cascade mechanism would entail interactions between neighboring scales. Thus the spectrum will be altered only by those interactions which have  $|k-k_1| \approx |k_1|$ . When  $|k-k_1| \approx |k_1|$  holds, the strength of the nonlinear interaction is weak if both  $\sigma_{k-k_1}$  and  $\sigma_{k_1}$  are of the same sign, i.e., either both are positive or both are negative. Thus, for copropagating waves, the nonlinearity is weak. It should be noted here, that unlike Alfvén waves, for whistlers the interaction between copropagating waves does not vanish identically, it is merely weak, in comparison to counterpropagating waves (i.e., when the two  $\sigma$ 's correspond to opposite signs). Thus the phenom-



enon of spectral wave cascade would be governed primarily by nonlinear interactions amongst counterpropagating whistlers.

The matching conditions for the frequency and the wave vectors for such kind of interaction can be written as

$$\pm \omega_3 = \omega_1 - \omega_2,$$

$$\mathbf{k}_3 = \mathbf{k}_1 + \mathbf{k}_2.$$

Here the suffix 1 and 2 refer to the two interacting whistler waves which generates a third whistler wave referred by index 3. Selecting positive sign before  $\omega_3$  and using the dispersion relation for whistlers we obtain

$$k_3 k_{3y} = k_1 k_{1y} - k_2 k_{2y}.$$

Now, we eliminate  $k_{3y}$  by using  $k_{3y} = k_{1y} + k_{2y}$ , which gives

$$\frac{k_{1y}}{k_{2y}} = \frac{k_3 + k_2}{k_1 - k_3}.$$

Now since  $k_1 \approx k_2 \approx k_3$ , the above-mentioned equation shows that  $k_{1y} \gg k_{2y}$  (choosing a negative sign before  $\omega_3$  would merely have resulted in the opposite inequality. This does not matter since 1 and 2 are merely dummy suffixes). Thus, instead of having  $k_{2y} \rightarrow 0$  as in Alfvén turbulence we have here  $k_{2y} \ll k_{1y}$ , which implies that there is very little cascade to small scales in the  $y$  direction. Cascade to small scales thus can occur only along the perpendicular direction. This explains the initial increase of  $\langle k_{\text{perp}}^2 \rangle$ .

The disparity in the average parallel and perpendicular scales in the asymptotic state can be understood by the following reasoning. Squaring the frequency matching condition and elimination of the vector  $\mathbf{k}_3$  leads to

$$\begin{aligned} & k_2^2 k_{1y}^2 + k_1^2 k_{2y}^2 + 4k_{1y}^2 k_{2y}^2 \\ &= -2k_{1y} k_{2y} [(k_1 + k_2)^2 + (k_{1y}^2 + k_{2y}^2)] \\ & \quad - 2k_{1x} k_{2x} (k_1 + k_2)^2. \end{aligned} \quad (5)$$

The positivity of the left-hand side of the Eq. (5) requires that the two wave vectors  $\mathbf{k}_1$  and  $\mathbf{k}_2$  have either both or one of the components of opposite sign. However, the natural tendency of power cascade in  $2d$  EMHD turbulence is toward short scales. Furthermore, both whistlerization and anisotropization of the spectrum are short scale phenomena. This, thus excludes the possibility of having both components of the interacting wave vectors of opposite signs. The comparison of the coefficients of  $2k_{1y}k_{2y}$  and  $2k_{1x}k_{2x}$  appearing in Eq. (5), then suggests that during the initial stages, when the spectrum is isotropic, the permissible interactions will predominantly have  $y$  components of the two interacting wave vectors as antialigned and  $x$  component as aligned. This results in preferential shortening of scales along the  $x$  direction (direction perpendicular to the applied magnetic field), and hence explains the dynamic development of anisotropy in the spectra. However, clearly this process is self-defeating. Once a certain disparity between the average parallel and perpendicular scales are developed, Eq. (5) can be satisfied by interactions amidst the wave vectors which lead to either the generation of short scales along parallel or perpendicular directions with equal likelihood. It can then be

expected that there will be no preferential shortening of perpendicular scales. The initial increase of  $\langle k_x^2 \rangle$ , which later stops growing, bears testimony to this scenario.

It is thus clear that the turbulent spectrum develops anisotropy in the presence of an external magnetic field basically due to a cascade mechanism mediated by whistler wave interactions.

## V. CONCLUSION

The role of normal modes of the system in determining the turbulent state and influencing the turbulent transport properties are now increasingly recognized. For this purpose, we have taken the specific case of the electron magnetohydrodynamics (EMHD) turbulence and investigated various aspects of whistlerization (whistlers being the normal mode of EMHD) of its spectrum.

We have introduced novel numerical diagnostics to quantify the extent of the whistlerization of the spectrum, and conclude that whistlerization is only partial. This has a direct bearing on the turbulent diffusivity of long scale magnetic fields. Recent works on quasilinear estimates of diffusivity have shown that the turbulent diffusivity would identically vanish if turbulent state is comprised solely of randomly interacting normal modes.<sup>8,12</sup> Our studies suggest that the short scale part of the spectrum tends to be more whistlerized, the long scales merely serving the purpose of providing an ambient magnetic field along which these normal modes propagate. It will indeed be a worthwhile exercise to carry out such studies at higher resolutions than what has been done here to draw conclusive and quantitative evidence of the phenomena of whistlerization at short scales, its Reynold's number dependence, etc. We also observe that the spectrum gets quantitatively more whistlerized with increasing strength of the external magnetic field. This is expected and is largely a consequence of reduced nonlinearity of the system in the presence of higher  $B_0$ .

There have been some recent attempts to invoke EMHD time scales to provide an explanation of the fast reconnection processes in the solar and astrophysical context.<sup>3</sup> Observational data on MHD scale fluctuations in solar wind indicates significant anisotropy.<sup>13</sup> Spectral anisotropy in the presence of long scale magnetic field in MHD has also been observed numerically and is being understood on the basis of a cascade mechanism governed by Alfvén wave interactions.<sup>9,10</sup> It is thus of interest to see whether, in the context of EMHD also, there is any dynamically generated spectral anisotropy in the presence of a mean magnetic field. Our numerical simulation clearly shows that the spectrum develops anisotropy in the presence of a uniform field along a particular direction. This can happen only if there is an asymmetry in the nonlinear spectral transfer process relative to the mean magnetic field. The only way nonlinear spectral transfer process could be asymmetric is if it is mediated by whistlers (as the dispersion relation, phase, and group velocities of these waves depend on the direction of the mean magnetic field). We have provided a theoretical explanation of the observed anisotropy on the basis of whistler wave interactions. This

confirms that whistler waves, the normal modes of EMHD model, play a crucial role in power cascade mechanism in a turbulent state.

Thus, to conclude we feel that “whistler effect” (whistler wave interactions influencing the power cascade mechanism) is present in EMHD turbulence. However, the manifestations of this effect is reflected largely in the subtle properties of cascade like anisotropy, etc., rather than on gross property like spectral index (where the effect seems to be either small or negligible). In this context it is worthwhile to point out that a recent numerical work on MHD turbulence also seems to rule out any modification of the spectral index due to the “Alfvén effect,” which was erstwhile widely believed to exist.<sup>14</sup> However, the dynamical development of spectral anisotropy, mediated by Alfvén waves interaction, in the presence of external magnetic field is well established. Thus, it is apparent that though the normal modes do indeed play a crucial role in power cascade mechanism, the ramification of this is not seen on gross properties like the power spectral index.

#### ACKNOWLEDGMENTS

We would like to thank the San Diego Supercomputer center, a National Science Foundation (NSF) funded site of the National Partnership for Advanced Computational Infra-

structure (NPACI) for providing computing time on the T90 supercomputer for this work. This research was partially supported by Department of Energy (DOE) Grant No. DE-FG03-88ER-53275.

<sup>1</sup>R. H. Kraichnan, *Phys. Fluids* **8**, 1385 (1965).

<sup>2</sup>A. S. Kingsep, K. V. Chukbar, and V. V. Yankov, in *Reviews of Plasma Physics* (Consultant Bureau, New York, 1990), Vol. 16.

<sup>3</sup>D. Biskamp, *Phys. Plasmas* **4**, 1964 (1996); D. Biskamp, E. Schwarz, and J. F. Drake, *Phys. Rev. Lett.* **75**, 3850 (1995); J. F. Drake, R. G. Kleva, and M. E. Mandt, *ibid.* **73**, 1251 (1994).

<sup>4</sup>D. Biskamp, E. Schwarz, and J. F. Drake, *Phys. Rev. Lett.* **76**, 1264 (1996).

<sup>5</sup>D. Biskamp, E. Schwarz, A. Zeiler, A. Celani, and J. F. Drake, *Phys. Plasmas* **6**, 751 (1999).

<sup>6</sup>A. N. Kolmogorov, *C. R. (Dokl.) Acad. Sci. URSS* **30**, 301 (1941).

<sup>7</sup>A. Das, *Plasma Phys. Controlled Fusion* **41**, 531 (1999).

<sup>8</sup>A. Das and P. H. Diamond, “Theory of two-dimensional mean field electron magnetohydrodynamics,” to be published in *Phys. Plasmas*.

<sup>9</sup>J. V. Shebalin, W. H. Matthaeus, and D. Montgomery, *J. Plasma Phys.* **29**, 525 (1983).

<sup>10</sup>S. Oughton, W. H. Matthaeus, and S. Ghosh, *Phys. Plasmas* **5**, 4235 (1998).

<sup>11</sup>D. Biskamp, *Phys. Fluids B* **1**, 1964 (1989).

<sup>12</sup>A. V. Gruzinov and P. H. Diamond, *Phys. Plasmas* **3**, 1853 (1996).

<sup>13</sup>W. H. Matthaeus, M. L. Goldstein, and D. A. Roberts, *J. Geophys. Res.* **95**, 20 673 (1990); V. Carbone, F. Malara, and P. Veltri, *ibid.* **100**, 1763 (1995).

<sup>14</sup>W. C. Muller and D. Biskamp, *Physics Abstracts physics/9906003 Jun* (1999).